# The International Intercomparison of 3D Radiation Codes (I3RC): Bringing together the most advanced radiative transfer tools for cloudy atmospheres

*R. F. Cahalan*[1], *L. Oreopoulos*[2,1], *A. Marshak*[1,2], *K. F. Evans*[3], *A. Davis*[4], *R. Pincus*[5], *K. Yetzer*[6], *B. Mayer*[7], *R. Davies*[8], *and I3RC participants*[*]

Submitted to the Bulletin of the American Meteorological Society

August 13, 2004

1.NASA GSFC, Laboratory for Atmospheres 2.JCET, University of Maryland Baltimore County 3.PAOS, University of Colorado 4.ISR-2, Los Alamos National Laboratory 5.NOAA-CIRES Climate Diagnostic Center 6.Raytheon 7.Deutsches Zentrum für Luft und Raumfahrt 8.JPL, California Institute of Technology

[*]Listed in Tables 1 and 2 of the manuscript

*Corresponding author:* Lazaros Oreopoulos, NASA GSFC, Code 913, Greenbelt, MD, 20771 USA. lazaros@climate.gsfc.nasa.gov, (301) 614-6128.

## Abstract

The interaction of clouds with solar and terrestrial radiation is one of the most important topics of climate research. In recent years it has been recognized that only full three-dimensional (3D) treatment of this interaction can provide answers to many climate and remote sensing problems, leading to worldwide independent development of numerous 3D radiative transfer codes. The "International Intercomparison of 3-Dimensional Radiation Codes", or I3RC, described in this paper, sprung from the natural need to compare the performance of these 3D radiative transfer codes used in a variety of current scientific work in the atmospheric sciences. I3RC is jointly funded by the US Department of Energy Atmospheric Radiation Measurement Program (DoE/ARM) and by the US National Aeronautics and Space Administration Radiation Sciences Program, and is also sponsored by the GEWEX Radiation Panel and the International Radiation Commission. I3RC intends to (1) understand and document the errors and limits of 3D methods; (2) provide "baseline" cases for future code development for 3D radiation; (3) promote sharing and production of 3D radiation tools; (4) derive guidelines for 3D radiation tool selection; and (5) improve atmospheric science education in 3D radiative transfer. Results from I3RC have been presented in two workshops and are expected to guide improvements in both remote sensing and climate modeling.


**Capsule:** An international Intercomparison of 3-dimensional Radiation Codes (I3RC) underscores the vast progress of recent years, but also highlights the challenges ahead for routine implementation of these codes in cloud, weather, and climate models.

Modeling of atmospheric and oceanic processes is one of the most important tools in Earth Sciences for understanding the interactions of the various components of the surface-atmosphere system and predict future weather and climate states. Great advances in computing power along with continuously decreasing costs at which it can be acquired have led to widespread popularity of computer models for research and operational applications. Naturally, output from models built for similar purposes are and will continue to be compared for research purposes by compiling results scattered in the scientific literature. In the last few years, however, such comparisons have emerged as more direct and organized efforts via centrally-directed intercomparison initiatives. Intercomparison of various aspects of atmospheric Global Climate Models (GCMs) is a good example of this (e.g., Cess, 1990), but it is also true for numerical codes focused on more specific atmospheric phenomena like Cloud Resolving Models (CRMs) which simulate cloud life cycles (Moeng et al., 1996). In the field of radiative transfer for climate and remote sensing applications, the most prominent intercomparison projects in the last few years are Intercomparison of Radiation Codes for Climate Models (ICRCCM) (Ellingson et al., 1991; Barker et al., 2003) and Radiation Transfer Model Intercomparison (RAMI) (Pinty et al.. 2001; 2003). The latter effort actually shares a unique feature with the subject of this paper, the International Intercomparison of 3D Radiation Codes (I3RC): it pertains to three-dimensional (3D) radiative transfer (RT). RAMI examines how solar radiation interacts with surface vegetation, while I3RC examines how solar and thermal radiation interact with cloudy atmospheres.

3D RT research in atmospheric sciences began with seminal work in the late 1960's and early 1970's in the Former Soviet Union (e.g., Mullamaa et al, 1972), expanded later in the 1970s (e.g., McKee and Cox, 1974; Davies, 1978) and has now become an independent and mature research area. We can broadly divide 3D RT investigations in cloudy atmospheres as targeting two major application areas: (1) remote sensing; and (2) radiative energy budgets.

The atmospheric and planetary science communities have known for along time that the remote sensing of cloud properties using current 1D RT is suspect because clouds vary horizontally, and it has been well documented since the EOS satellite era that 3D RT effects are important and ubiquitous. Indeed, over the past decades significant errors in plane-parallel (1D) cloud retrievals have been documented using increasingly realistic models of 3D cloud structure (e.g. Cahalan, 1989, Chambers et al., 1997; Várnai and Marshak, 2002). A large part of the motivation for accurate remote sensing of cloud properties is that clouds play a major role in climate dynamics (e.g., Ramanathan et al., 1989; Fu et al., 1995; Kiehl and Trenberth, 1997), so modelers need to know whether they are adequately represented in GCMs.

The cloud and climate modeling community is further ahead of its remote sensing counterpart in incorporating the advances of 3D RT into its representation of radiative processes. This is not only because a forward problem is almost always more tractable than an inverse problem, but also because GCMs are only interested in large-scale averages of angularly-integrated radiation fields —boundary fluxes and internal heating rates. Such coarse radiation fields are faster to calculate and less error-prone than the angularly and spatially detailed radiances (i.e., “pencils” of radiation) of interest in remote sensing. Despite this advantage, there is still much room for improvement in how GCMs should account for the unresolved variability of cloudiness inside each grid-cell at both solar and thermal wavelength. The Independent Column Approximation (ICA) is presently the most popular framework for improving GCM parameterizations of broadband (spectrally-integrated) RT. ICA radiatively resolves subgrid variability by averaging results for individual vertical columns, but does not allow for radiation to be exchanged between columns. Its popularity and usefulness stems from the fact that, for many different cloud types and conditions, it gives domain-average results that are close to the full 3D results (e.g., Cahalan et al., 1994; Barker et al., 1998; Barker et al., 1999). However, as new modelling breakthroughs such as the Multiscale Modeling Framework (MMF) or "superparameterization" (Randall et al., 2003) make explicit representation of subgrid cloudiness a reality, it is no longer obvious that certain aspects of 3D RT can be safely ignored. In other words, MMF cloud fields may be too highly resolved in the near future (~1 km) that neglecting the radiative interactions between cloudy columns will be blatantly unrealistic.

The goal of I3RC is to promote the improvement of algorithms used for 3D radiative transfer in cloudy atmospheres. Activities do not only include comparisons of results from state-of-the-art 3D radiative transfer codes, but also development of fast approximations more suitable for climate or educational purposes, and commmunity "open source" codes that distill the best current knowledge on how to treat the various interactions of ultraviolet, visible, and infrared photons with atmospheric constituents. As such, I3RC is expected to be beneficial for practitioners of atmospheric radiative transfer in the modeling (GCMs, CRMs, etc.) and observational (e.g., remote sensing) community. More specifically, I3RC was conceived to:

- address the importance of accuracy requirements.
- contribute to error detection and improvement in the participating codes.
- delineate acceptable error tolerance for radiation quantities that are the cornerstone of remote sensing from space (i.e., radiances).
- reveal requirements for future generation surface cloud-probing instruments with respect to resolution, accuracy, mode of operation, etc.
- guide the development of techniques that produce or predict sub-resolution variability.

- generate momentum for continuing and expanding observational and modeling efforts that generate three-dimensional cloud fields.

I3RC is jointly funded by DoE's ARM program and by NASA's Radiation Sciences Program, and is also sponsored by the GEWEX Radiation Panel and the International Radiation Commission. It is proceeding in 3 phases. The first two phases have been largely completed, and will be further discussed in sections that follow. Workshops have taken place to discuss the results and lessons learned from each phase. Phase 3 is currently underway. It will use 3D cloud fields reconstructed from combined simultaneous observations of Terra instruments (possibly ASTER, MISR and MODIS) and will emphasize improving, extending, and sharing radiative transfer modules, aided by working groups on "Approximations" and "Open Source". The "Approximations" group, led by Anthony Davis, considers both deterministic and stochastic approximate methods in an attempt to gain advantages in execution time, and also to advance the understanding of 3D radiation processes for eventual implementation of these algorithms into other models. The "Open Source" subgroup, led by Robert Pincus, is developing a Monte Carlo (MC) radiative transfer code in Fortran-95 that makes state-of-the-art techniques available to a wide range of users. Activities of both subgroups are further explained in two subsequent sections.

**TODAY'S DOMINANT 3D RT TOOLS.** Before discussing the two completed phases of I3RC we would like to step back for a moment and briefly introduce to the reader the two 3D radiative transfer tools that are currently dominating atmospheric radiation applications, namely the Spherical Harmonic Discrete Ordinate Method (SHDOM) of Evans (1998) and the Monte Carlo (MC) method (Marchuk et al., 1980). These two methods while being completely different in their approach for solving the 3D radiative transfer problem, are the only options currently available for dealing with the full suite of problems put forth by I3RC.

SHDOM (Evans, 1998 for details) is the most widely used explicit multi-dimensional radiative transfer model in the atmospheric sciences. This is probably because it is highly efficient, very flexible for atmospheric radiation problems, and publicly available. SHDOM uses both the spherical harmonic and discrete ordinate representations of the angular aspects of the radiation field during different phases of the solution procedure. The spatial part of the fields is represented with a grid. Discrete ordinates are chosen because they more physically model the streaming of radiation through space. Spherical harmonics are chosen because they are more efficient for computing the scattering integral in the radiative transfer equation (RTE) and can more compactly represent the radiation field. Rather than storing radiances, SHDOM stores the source function with a spherical harmonic series at each grid point. The radiance field can be obtained easily from the source function with the integral form of the RTE. The length of the spherical harmonic series is adaptive, meaning that the truncation level varies from grid point to grid point. Only a few terms of the series are needed if the grid point has no scattering, the scattering is smooth (e.g. isotropic or Rayleigh), or the radiance field is smooth (e.g. inside optically thick scattering media). Moreover, SHDOM incorporates adaptive gridding, i.e., it puts a finer grid where needed. This reduction of memory usage is critical for 3D problems that take tens to hundreds of millions of numbers to represent the radiance field. The SHDOM solution method is source iteration, which is the usual approach for the discrete ordinate method.

Monte Carlo (MC) methods are a general technique for constructing probabilistic models of real processes. In contrast to SHDOM which solves the RTE explicitly, MC achieves the same statistically. In its application to radiative transfer in the atmosphere, MC computes the flow of radiation by simulating the trajectories of photons emitted from a source such as the sun for shortwave radiation or the surface and cloud elements for longwave radiation. The trajectories are determined probabilistically: the distance between interactions with the medium, the probability of being absorbed, and the direction of travel after each interaction are determined for each photon by comparing random numbers with probabilistic representations of the atmosphere's optical properties (extinction, single scattering albedo, and scattering phase function). MC methods are valuable because they are exceedingly flexible and because the error in the final estimate of radiative quantities can be predicted by examining the variance between estimates made from subsets of the simulation.

In "straightforward" Monte Carlo the radiative quantities of interest (i.e. fluxes, heating rates, radiances) are determined by counting the fraction of photons that meet a certain fate: domain-averaged reflectance, for example is the fraction of photons that exit from the top of the domain. The straightfoward approach is very simple but, as I3RC has confirmed, it is impractical for the solution of complicated problems, such computing the spatially-dependent radiance field above a variable patch of clouds and reflective surface. The difficulty has several causes, including the strongly-peaked scattering phase functions exhibited by cloud drops and the multiple scattering that occurs in optically dense media like clouds. The former increases the variance of the MC estimate while the latter increases the execution time of MC codes. To improve MC performance, techniques such as "maximum cross section" and "local estimate" have been suggested to reduce variance and speed up MC runs. Both methods are described in the 25-year-old monograph by Marchuk et al. (1980), which remains the single best reference on the Monte Carlo simulations of radiative transfer in the atmosphere. They are gaining popularity, as Tables 1 and 2 show, because they speed up some classes of calculations and make others possible.

**I3RC PHASE I.** During Phase I, now complete, several baseline 3D radiative transfer computations on three cloud fields were performed. The three cloud fields were an academic 1D "step" cloud field, a 2D field derived from the ARM cloud radar, and a 3D field derived from radiances measured by the Landsat 5 Thematic Mapper instrument (Fig. 1). In November 1999, participating members of 17 research groups, representing several countries and 22 different 3D algorithms, met in Tucson, Arizona USA and compared their results for the various experiments of Phase I. The computations were monochromatic (single-wavelength, not explicitly specified), with droplet scattering and absorption only (no emission), and involved cloud and Earth-surface effects only. They were completed independently at the participants' home institutions. Results of these computations are summarized on the I3RC web page (see later section) at *http://i3rc.gsfc.nasa.gov* while highlights will be detailed in a forthcoming paper.

*The participants*. Results for at least one experiment (although not necessarily the complete set) were submitted for 22 different models. Table 1 lists the codenames of the participating groups, the institution reflecting affiliation at at the time of submission, the principal researcher responsible for code development and result submission, and a brief characterization of the algorithm type. The table contains 23 entries because UCOL participated with dual submissions corresponding to two different angular resolutions for an otherwise identical SHDOM (Evans, 1998) code.

*Cloud fields, requested output, and submission strategy*. Three cloud fields of a wide degree of size and complexity, and therefore computational strain were selected. These cases were designed so that on one hand a large number of 3D modelers would be attracted to the project by being able to run at least one case, but also so that some participating models would be tested to their limits in terms of computation time and memory use. Molecular and aerosol scattering or absorption were not considered in the first phase in order to simplify the provided package of input data and to ensure that any differences were restricted to the treatment of cloud-radiation interactions.

**Case 1**, called "step function cloud" or "square wave cloud" was the simplest cloud field (Fig. 1, top) consisting of 32 columns (pixels) of equal width along the $x$-direction, the first 16 having an optical depth of 2 while the remaining had an optical depth of 18. The size of the entire field was set to 0.5 km. The geometrical thickness of the cloud (along $z$-axis) was set to 0.25 km everywhere (flat-top cloud) and the extinction coefficient was assumed to be homogeneous in the vertical. The cloud had infinite extent in the $y$-direction and periodic boundary conditions were set for the $x$-direction (photons exiting either of the sides of the cloud reappear on the other side). Obviously, this is an academic/pedagogical example where the main interest lies in examining model behaviour around the region of optical thickness transition.

**Case 2**, called "Radar cloud" was a cloud field based on extinction retrievals from the MMCR (Millimiter Cloud Radar) and the MWR (microwave radiometer) at the ARM CART site in Lamont, OK on Feb. 8, 98 (Fig. 1, middle). These retrievals were performed by Sally McFarlane, now at PNNL, and kindly provided to us by Frank Evans. The field consisted of 640 columns along the $x$-direction, each of which was set to have a 50 m horizontal width and was vertically resolved into 54 vertical layers of 45m thickness ($z$-direction). For our radiative transfer calculations we assumed the cloud to be infinite along the $y$-direction and periodic in the $x$-direction.

**Case 3**, called "Landsat cloud" was a cloud field from an Independent Pixel Approximation retrieval on a 128x128 subregion of a Landsat-4 scene used in Oreopoulos and Davies (1998), and provided kindly by Bruce Wielicki of NASA Langley (Fig. 1, bottom). Each pixel was $(30m)^2$. Details on retrieval assumptions and the statistics of the derived optical thickness field can be found in the I3RC website.

An exhaustive description of the all Phase I experiments is provided in the I3RC website. To summarize here, there were 4 experiments for cases 1 and 3, and 8 experiments for case 2. Case 1 and 3 experiments involved changes in illumination (Sun) angle and single scattering albedo, and case 2 experiments involved changes in illumination angle, single scattering albedo, scattering particle phase function, and surface albedo. The requested output were fields of boundary fluxes, horizontal flux, nadir bidirectional reflectance, zenith bidirectional transmittance (whenever the sun was not overhead), bidirectional reflectances at 60° view, errors to the mean of all the above quantities, and CPU time for each experiment along with the technical specifications of the computer(s) used to run the simulations.

Participants submitted most of their results by a predetermined deadline without having access to the results of their colleagues. However, assistance was provided by the NASA/UMBC research group leading the effort who made quick-look quality checks of the submissions: whenever spurious results were identified or implementation errors were suspected, participants were alerted to double-check that experiments were run according to instructions. If a problem was indeed detected, resubmission of revised results was allowed within a short grace period.

*Comparison methodology*. The obvious problem of intercomparison exercises like I3RC is evaluating the absolute accuracy of the models since true answers are not available. However, this is not always necessary since the goal of intercomparisons is usually not to find the best model, but to identify the spread of submitted results. GCM intercomparisons are good examples of this (Cess et al., 1989; 1990; 1996). Nonetheless, when all participating models are known to use approximations to model the cloudy atmosphere, the availability of benchmark results ("truth") from a model that does not (to the greatest degree possible) make approximations is extremely useful and instructional. Such was the case in an intercomparison of 1D GCM radiative transfer algorithms where 3D benchmark results were available (Barker et al., 2003). I3RC falls somewhere in the middle, having to face challenges similar to RAMI (Pinty et al., 2001; 2004). Rather than developing comparison metrics that provide an overall measure of model performance over a number of experiments and conditions, results were generated which allow the comparison of a specific model to all others *for each* case, experiment, and radiative quantity. More specifically the models were compared from estimates of:

- Their first three moments (mean, standard deviation, skewness)
- Cross-correlations with one of the participating models (UMBC1).
- Root mean square (rms) deviations from one of the participating models (UMBC1).
- The median of the absolute deviation from one of the participating models (UMBC1).

Visual comparisons were also made by plotting fields (or partial fields) and (for case 3) histograms of the various radiative quantities derived from the full fields. The subsequent development of interactive tools for plotting (see section 6) allowed more flexibility on model intercomparison. For example, cross-comparison statistics can now be calculated with respect to any participating model or the "consensus" mean field.

*Results*. The complete collection of results can be found in at the I3RC website, while more in depth analysis of some selected results will be published in a forthcoming paper. Here we provide only a couple of examples to give the interested reader an idea of how the intercomparison was conducted and what a typical level of agreement was.

Fig. 2 shows reflectance ($R$), transmittance ($T$), absorptance ($A$) and horizontal flux $H$=1-$R$-$T$-$A$ for experiment 4 of case 1 (step cloud). The single scattering albedo (probability of a photon surviving after an interaction with the cloud particle) is 0.99, the scattering phase function is that of Henyey-Greenstein with asymmetry factor (mean cosine of the scattering angle) $g$=0.85, the solar zenith angle is 60° (Sun shining from left), the surface is black (non-reflecting), and periodic boundary conditions in the horizontal are used. 18 codes participated in this experiment, but only the models that are outliers are identified. Both outlier models use approximations to calculate the radiative fluxes: LANL1 uses diffusion theory to approximate multiple scattering, while MESC2 is a regular MC code which uses δ-scaling of optical properties for all portions of the cloud below 1 optical depth from the cloud top in order to accelerate computations. All other models are barely distinguishable for all three components of the flux field ($H$ is only a residual). Note that the horizontal flux $H$ is only different from zero in a real three-dimensional application (e.g., Marshak et al., 1999) and is therefore a good measure for cloud inhomogeneity and the capability of the different models to treat it correctly (due to energy conservation $H$=0 for domain-averages even for 3D).

Fig. 3 shows nadir radiance (bidirectional reflectance) fields of selected submissions for experiment 4 of case 3 (the Landsat field of Fig. 1). The input parameter values are the same as in the step cloud case shown before. It can be seen that all participants capture the main spatial features of the radiance field, while for the MC fields (all but UCOL1) the noisiness of the field is a function of the number of photons used and the method of radiance calculation, i.e., "cone" method (e.g., Várnai and Davies, 1999) vs. "local estimate" method (e.g., Marshak et al., 1995). It should be stressed, however, that even the noisest of the submissions manage to capture the mean radiance field quite accurately. This is demonstrated in Fig. 4 which shows the mean radiance field of each submission. Only two fields differ by ~0.01 (~3.5%) from the consensus mean, while the noisiest field (UNIK) appears to be very close to the consensus mean even though it has by far the largest standard deviation.

*The Phase I workshop*. The Phase I workshop took place in Tucson, AZ, 17-19 Nov., 1999. The workshop was the first opportunity for participants to see how their results compared with those of others. Separate sessions were organized to present the performance of the models for each of the cloud cases. One individual was designated to perform the intercomparison analysis for each session, but a group discussion followed each presentation. Based on these presentations some participants requested that they be allowed to review their calculations in order to eliminate the possibility of erroneous interpretation of input or requested output and to reexamine the robustness of their codes. It was decided that an additional three month period be granted for resubmission of results for those who optioned to make another round of computations. The results currently posted at the I3RC website and those shown in Fig. 2-4 are the final submissions after this 3-month grace period. In addition to the sessions focused exclusively on the main objective of I3RC, there were also other sessions on various aspects of 3D radiative transfer where speakers made presentations on such diverse topics as the effects of 3D on shortwave cloud absorption, stereo cloud retrievals from space, radiative transfer in mixed phase clouds, ultraviolet radiative transfer under cloudy conditions, line-by-line (high spectral resolution) 3D radiation codes, and others. Extended abstracts describing the participating models can be found in Cahalan and Davies (2000).

**PHASE II.** In Phase II of I3RC, more complex computations were requested for two broad application areas, “remote sensing” (dealing mainly with radiances) and “heating rate”. The computations were performed on a stratiform and a convective cloud field, each simulated with a different LES model (Fig. 5). Phase II computations included effects of gases and aerosols in some experiments and occasionally ventured into thermal wavelengths. During Phase II, participating groups were asked to port their code to a Linux workstation provided at NASA-GSFC. This allowed timing comparisons, and facilitated contributions to an "Open Source" public library for solving 3D radiative problems. Results of Phase II computations can also be found at the I3RC website, while a detailed description of the exercise and a summary of the most important results is also planned as a separate paper.

Differences from Phase I include the incorporation of atmospheric absorption and scattering in some experiments, the presence of non-lambertian surfaces in selected experiments, the requirement for broadband calculations in some experiments, the inclusion of experiments with realistic remote sensing conditions (off-nadir bidirectional reflectivities were asked at multiple angles), and the calculation of internal heating rates. As mentioned above, another innovation was setting a goal to perform a small subset of experiment on a common computer platform at GSFC so that assessments of the computational requirements and speed of the various models can be obtained.

*The participants*. In part due to the more complex nature of the cloud fields and experiments in Phase II, fewer codes (13) participated compared to Phase I. Other than MC, only SHDOM participated in this phase. The list of participants can be found in Table 2.

*Cloud fields, application areas and experiments*. Phase II consisted of two main application areas:

- Radiance fields for cloud remote sensing.
- 3D heating rate fields for large eddy simulation model parameterization.

A detailed listing of the experiments is provided in the I3RC website. All experiments were run for two different numerical accuracies, “high” and “low” (i.e., numbers of photons for MC methods). CPU time was reported for a subset of these experiments. This allowed evaluation of the CPU time/accuracy tradeoff for the participating models in the different types of experiments. Only those outputs appropriate for the application were computed. This reduced complexity in submissions and comparisons, and kept the focus of the intercomparison on the applications.

All experiments are run for two LES model cloud fields a cumulus case and a stratocumulus case (Fig. 5). LES model output has been selected for convenience as it provides full 3D cloud fields. The two cloud fields were:

**a) cumulus (Cu)** cloud field from Bjorn Stevens LES modeling (Stevens and Lenschow, 2001) of the GCSS continental shallow cumulus boundary layer (ARM Oklahoma site) experiment (Fig. 5, top) The cloud field consists of 100x100x36 cells with gridsize 66.7m X 66.7m X 40m. For more details on this cloud field the interested reader is referred to the I3RC website.

b) **stratocumulus (Sc)** a field from Chin-Ho Moeng LES modeling (Moeng et al., 1996) of the FIRE-I stratocumulus experiment, see (Fig. 5, bottom). The cloud field consists of 64x64x16 cells with gridsize 55m X 55m X 25m. For more details on this cloud field the interested reader is referred to the I3RC website.

*Comparison methodology*. A main difference from the comparison methodology used in Phase I was that instead of picking a particular model as the "measurement stick", the consensus results of the participating models were used as the benchmark ("truth"). In other respects the analysis of the submissions was carried out in a manner similar to Phase I.

*Results*. The complete collection of results can be found in at the I3RC website, while more in depth analysis of some selected results will appear in a forthcoming paper. Here, we provide only one characteristic example. It is given in Fig. 6 which shows nadir reflectance fields for Exp. 7 applied on the LES Cumulus cloud field. This experiment includes an absorbing and scattering atmosphere consisting of aerosols and gases, a reflecting Lambertian surface, and assumes a Mie phase function for the scattering particles (spherical liquid droplets, non-absorbing for this experiment). The sun is at a solar zenith angle of 60° and is shining from the left side of the domain. It can be seen that only a few participants submitted results for this case (7 participants with 8 codes) suggesting that at the time, some of the codes did not have the capability to deal with a case of such a level of complexity: for Experiment 2 which was otherwise identical to experiment 7, except for the omission of atmospheric effects, 12 submissions were available. Nevertheless, it was encouraging to see that there was quiet good agreement among the models that did participate in Exp. 7, notwithstanding an expected increase in divergence as comparisons extended to higher moments (Fig. 7 shows only the mean and standard deviation). The level of agreement shown in Figs. 6 and 7 was typical of the level of agreement for other Phase II experiments.

*The Phase II workshop*. The second I3RC workshop also took place in Tucson, AZ on November 15-17, 2000. While the central focus was on the Phase II results which were presented for the first time to the invitees, there were also other sessions on current 3D issues pertaining to radiative transfer in clouds, such as handling cloud heterogeneity in GCMs, impact of 3D effects on remote sensing of clouds, computational techniques adapted from other fields, etc. There were also breakout sessions for the "Approximations" and "Open Source" intitiatives (see next two sections), a planning session on upcoming (Phase III) computations, and a roundtable discussion on the future of I3RC as well as on products and tools that I3RC can make available to the wider community. Abstracts describing the participating codes and their approach for tackling the experiments of Phase II can be found in Cahalan and Davies (2000).

**APPROXIMATION METHODS FOR 3D RADIATIVE TRANSFER.** This subtask of I3RC, headed by Anthony Davis, was conceived in broad terms during a break-out session at the first I3RC Workshop and its purpose was further refined in discussions at the second I3RC Workshop. It has sprung from a desire to make available to 3D practitioners alternative algorithms to MC and SHDOM which currently dominate as prime choices for attacking even the simplest 3D RT cloud problems This section defines what falls under the category of "Approximation Methods", describes the related subtask and summarizes its goals and achievements thus far. At the time of this writing, it is fair to say that the "Approximations" subtask is far less advanced than the comparison between exact methods (which is itself dominated by MC methods). This is because (1) the atmospheric RT community is relatively new to the art of approximation in computational 3D transport theory, and (2) the challenges are considerable, while the allocated resources are still meager. It is nevertheless instructional to discuss in some more detail what the subtask is about, what its goals are, and how I3RC plans to achieve them.

In general, two distinct categories of approximate/fast 3D radiative transfer models can be defined:

• "approximate deterministic" models, directly comparable to the bulk of computational techniques represented in I3RC considered “exact” in the sense that they are all solutions of the same 3D radiative transfer equation.

• "approximate probabilistic" models, which do not use all the standard I3RC input nor predict much beyond the domain-averages of a few I3RC output fields.

I3RC managed to compile extensive but probably not exhaustive lists of models in each category, with short descriptions and tentative names. Each of the models was mapped to one or two individuals considered responsible for its origination or maintenance; see Tables 3 and 4.

*Deterministic*. The first class of models has a natural place in I3RC because they produce radiation fields for given extinction fields and thus can be directly compared to "exact" methods. The difference is that they numerically solve simpler sets of equations and therefore are expected to be orders of magnitude faster than MC and even explicit methods of solving the full-blown 3D RTE such as SHDOM (Evans, 1998). A well-known example is 3D diffusion theory (e.g., Davis and Marshak, 2001) which can be derived from the RTE in a variety of ways, and these derivations give us insight into where the approximation should and should not work. An evolving list of 14 possible candidate models in no particular order is given in Table 3. There are two levels of accuracy to ascertain:

- The *physical* accuracy of the alternate model (how well the simplified model approximates exact radiative transfer theory).
- The *mathematical* accuracy of the implementation (how well we are numerically solving the new simplified equations).

The prime application for this type of model is a situation such as dynamical cloud modeling (LES- or CRM-style) where computer time is a concern for every proposed enhancement. Another, longer term, application would be computer-aided cloud optical tomography where cloud shape and structure would be varied to fit a number of observations, i.e., fully 3D cloud remote sensing.

Development and intercomparison of these codes is an ongoing effort which benefits largely from the I3RC benchmark calculations. Modelers are encouraged to use the same cases as in Phase I to produce the same outputs, starting with the simpler ones (fluxes) and then proceeding to the more difficult ones (radiances). However, the eventual goal is to have these models tackle the cases of Phase II since they were designed purposefully to be very close to the level of detail required in the targeted applications.

*Probabilistic*. The second class of models makes no attempt whatsoever at predicting the specifics of radiation fields for some extinction field, but estimates only domain averages, possibly even only ensemble averages of the domain average. Here the extinction field is only used in some kind of statistical preprocessing to numerically determine the one or more variability parameters that these models all possess, since they all have a probabilistic flavor. Then the approximate radiative transfer calculation per se is performed, hopefully in hardly more time than the typical 2-stream computation performed in GCMs. Table 4 provides a list of 12 possible candidates, in no particular order.

Most of these models can be viewed as radiative parameterizations for GCMs in the early design phases: they target the large-scale properties of interest in climate studies but some of them are not yet broadband or multi-layer capable. Since probabilistic models are generically based on some conceptual idea of how 3D cloud variability affects the overall patterns of radiation transport, another potentially important application for them is for them to simply be diagnostic tools for interpreting data (appropriately averaged to some relevant scale). For instance, these simple models can help to sort real-world situations into more and less variable cases. From there, the models can help to make predictions on other observable quantities and/or to plan new measurements.

Intercomparison of these codes is still in the planning stage. There are three basic problems that need to be addressed before any organized intercomparison effort: (1) How much data is needed to define model parameters? (2) How representative is an ensemble-mean with respect to a single realization? (3) What are the radiative properties that are targeted? Some of these issues were also raised by Kassianov et al. (2003).

**MC OPEN SOURCE INITIATIVE.** The two most widely used tools in atmospheric radiation today are the Discrete Ordinate Method (DISORT, Stamnes et al., 1988), available via anonymous ftp at ftp://climate.gsfc.nasa.gov/wiscombe/Multiple_Scatt/ and SHDOM, publicly available http://nit.colorado.edu/~evans/shdom.html. Both are algorithms developed thanks to the courageous efforts of only a handful of individuals (Evans in the case of SHDOM and Laszlo/Stamnes/Tsay/Wiscombe in the case of DISORT). These individuals were responsible for developing, testing, documenting, distributing, and supporting their algorithms with little or no help by the RT community at large (except for the occasional detection of minor bugs by users).

The "open source" initiative within I3RC takes a different approach by developing the framework of a MC model for solving radiative transfer problems in inhomogeneous cloudy atmospheres, and expecting contributions from the 3D RT community worldwide to complete the development of the full code. I3RC thus provides a baseline code that is flexible and robust, and useful in both teaching and research contexts, but which in its initial release computes only monochromatic domain-averaged reflected and transmitted fluxes and their uncertainty estimates. As already stated, this code will provide the platform for further developments, and the hope is that the I3RC community will contribute by adding modules for other features (radiance and heating rate calculations, spectral integration, etc.)

We have tried to build a framework that can provide pieces of code that can be re-used in MC and other radiative transfer codes. To that end, we have followed software engineering practice and defined a set of modules, each of which represents some portion of the problem. Each module is defined by one or more data structures and a set of procedures (functions and subroutines) that operate on those structures. The modules build on one another, but are structured so that any module can be replaced by another implementation, as long as the new provides the data structures and procedures we have defined. These modules are written in standard Fortran 95, which we hope will strike a good balance between efficiency and portability.

As a concrete example, we have defined a module to represent a “scattering phase function” that describes how light striking an individual particle is re-distributed with respect to angle. Phase functions are usually described either as a set of values as a function of the scattering angle, or as the coefficients in a Legendre polynomial expansion. Our module defines two data structures, one to store a single scattering phase function and one to hold a set of such phase functions (so that it's easy to represent how the phase function varies with particle size, for example). There are procedures to define a phase function, write it to or read it from disk, determine the value of the phase function at some arbitrary angle, determine the Legendre coefficients, and so on. The phase function may be defined initially as either angle-value pairs or as Legendre coefficients, but this is transparent to users thereafter. The phase function module is required by the module that defines the optical properties within a domain, as well as by others more specifically related to MC.

The nucleus code contains this framework, some associated infrastructure (i.e. translators from other frequently-used file formats), and integration subroutines for monochromatic fluxes with Lambertian surface properties. We have tested the code for all the I3RC Phase I cases. We hope that research interests within I3RC will produce communal efforts to include integrators to compute radiances and to add thermal sources so the model is more helpful to the longwave remote sensing and modeling practitioners. Extension to backwards MC (as would be used, for example, to calculate the flux observed by a ground-based pyranometer for different illumination conditions or as an alternative to the forward model for thermal calculations) is also desirable and is part of our future plans.

Beyond its obvious utility as a classroom/course tool, we anticipate that the I3RC MC "open source" model will benefit the atmospheric science community by providing:

- Tested documented benchmark code for 3D radiative transfer problems

- A structure to facilitate development of new radiative transfer solvers
- A modular "laboratory" to compare and improve MC algorithms.

**The I3RC WEB SITE.** The process of organizing, advertising, running, and assessing I3RC would have been significantly more strenuous were it not for the widespread use of the internet and the World Wide Web. A dedicated website, *http://i3rc.gsfc.nasa.gov* has been used to provide general information on the project's goals and plans, scheduling, documentation and instructions for the experiments, and most importantly to present analysis of the results submitted by the participants.

Here, we describe briefly the most popular feature of the website, namely the interactive tool that displays the results from both phases of I3RC. This tool generates plots (e.g., box/bar plots, X-Y plots) of either statistics (e.g., means, standard deviations, skewnesses) or fields from the data provided by the I3RC participants. The routines are written in the java programming language and thus allow for a certain degree of user input (i.e., the user has some control both over the values displayed and the appearance of the plot). In addition, they include the capability of exporting individual plots into postscript files on the local machine that can then be sent directly to a printer. Visitors of the web site who want to view results still have the option to use links that provide access to static plots (user has no control over the plots).

Figure 8 shows two of the menus of the interactive tool for Phase I results, the top is for the summary statistics (mean, standard deviation, skewness) and the bottom is for cross-comparison statistics (rms errors, cross-correlations, medians of absolute deviations). The user can choose the case of interest, the experiment (non-applicable experiments for a particular case are grayed-out), the desired quantity to be displayed (non-applicable quantities for a particular case and experiment are grayed-out), the desired statistic, whether or not to include the approximate methods in the plots, etc. The cross-comparison statistics menu (Fig. 8, bottom) offers the choice of comparing the results of one or more participants to the ones of a specific participant, or the consensus mean (either with or without the results from the approximation methods) in terms of spatial (field) cross-correlation coefficients, the rms of the spatial differences, or the median of the absolute deviation differences. Some other self-explanatory choices for displaying the results can also be seen.

Finally, there is an interactive tool that can produce plots of the radiation fields calculated by the participants for the various experiments of I3RC. The menu for this tool is shown in Fig. 9. Important features of this tool are that it can also plot difference fields between a selected participant and any other participant, including the consensus mean field (with or without the results of approximate methods included; with or without the outliers included), and that it can extract a specific row and column that the user specifies for 2D fields (Case 3 of Phase I and the two cases of Phase II).

It can thus be seen that the wealth of I3RC results can be controlled to a large extent by the user of the interface. This is obviously of great usefulness to the user who happens to also be a participant in I3RC (or simply a third-party user of one of the codes that participated) since he/she can focus on the performance of a particular code.

**CONCLUDING REMARKS AND FUTURE OF I3RC.** Under funding from NASA's Radiation Sciences and DoE's ARM programs, the first two phases of I3RC have been largely completed, with the third phase currently in progress. Two successful I3RC workshops with international participation were held in Tucson, Arizona and a website dedicated to the project has been developed (http://i3rc.gsfc.nasa.gov). The first two phases of I3RC had as a main goal to evaluate the performance (accuracy and computational efficiency) of a wide variety of 3D radiation codes. Participants performed well-defined radiative experiments of varying complexity with a set of cloud cases, beginning with an academic “step cloud” and proceeding to more realistic cases. These experiments addressed the impact of 3D cloud structure and radiation interactions for both radiation budget and remote sensing problems.

In Phase I, 22 different codes from 15 institutions performed solar experiments for at least one of three cloud cases (one academic, one reconstructed from MMCR observations and one inferred from Landsat retrievals). Solution methods ranged from the popular MC technique, to the publicly available solver SHDOM, to 3D diffusion and discrete angle approaches. Intercomparison of the first-round of submissions took place during the first I3RC workshop and helped several participants to identify problems with their codes. The close agreement among models after the second round of submissions is a testament of the valuable role of I3RC in the detection of coding errors and overall 3D algorithm improvement.

Phase II cloud cases were obtained from two LES models. Another change compared to Phase I was the inclusion of molecular and aerosol scattering and absorption and of selected experiments at thermal infrared wavelengths. Both the domain sizes and the design of the experiments themselves raised the degree of difficulty compared to Phase I. As a result, fewer codes participated (SHDOM and 12 MC codes). This fact, by itself, has underscored the challenge faced by non-MC, non-SHDOM approaches for becoming capable to tackle realistic problems most relevant to remote sensing and climate applications. Results for Phase II were presented in the second I3RC workshop. Final results can now be viewed as both static and interactive plots at the I3RC website. Agreement between participating codes was in general very good. Given the vast number of produced radiation fields, the analysis of the impact of 3D cloud structure under different illumination and viewing geometries remains to be completed, and will be further detailed in forthcoming papers dedicated to each I3RC phase. Since all results are available to the public, interpretation of the I3RC ouputs can potentially become a collective exercise of the 3D radiation community.

Phase III will employ 3D cloud fields reconstructed from advanced retrieval techniques on common field of view observations of two or more NASA Terra radiometers, will extend the computations to “searchlight” and lidar-type experiments, and will emphasize improving and sharing radiation code, aided by working groups on "Approximations" and "Open Source". The "Approximations" group considers both deterministic and stochastic approximate methods in an attempt to gain advantages in execution time, and also to advance the understanding of 3D radiation processes. The "Open Source" subgroup will develop a MC radiative transfer model that makes state-of-the-art techniques available to a wide range of users.

Similar to RAMI (Pinty et al., 2001; 2004), its sister 3D project focusing on vegetated surfaces, I3RC has accomplished a great number of its goals such as (1) invigorating interest on current 3D radiative transfer issues in the atmospheric sciences community; (2) providing useful benchmarks for code verification and development; (3) helping in identifying weakness or even bugs in 3D algorithms, and (4) leading the way in 3D “open sourse” algorithm concepts. At the same time, I3RC has faced a number of challenges, some of which it is well underway in meeting, and some for which additional efforts will be required. Some of these challenges are:

(1) ***Diversity of methods***. Participating methods that solve the exact 3D transfer equation on grids include 3D discrete ordinates, and SHDOM. All of the other participating methods are based on MC techniques. These include several versions of MC – forward, backward, and

conjugated adjoint. Many MC codes share similar techniques, such as maximum cross section, for speed and variance reduction. MC approaches solve the exact radiative transfer equation, and have relatively well-understood errors, so they are useful in evaluating errors of other methods. 3D methods that begin by approximating the transfer equation, such as diffusion and discrete-angle methods, also participate in I3RC, and can often gain speed advantages over the exact methods, sometimes at the expense of significantly larger errors. Since 3D approximations were absent in Phase II of I3RC, more efforts shall be made to meet the challenge of diversity.

(2) ***Applicability***. For I3RC to benefit both remote sensing and climate modeling, it is necessary for I3RC computations to include a wide variety of radiances, fluxes, and heating rates. Outputs quickly multiply. Even the restricted set of fields and outputs of Phase I led to ~1000 comparison plots. For these to be useful and accessible requires a simple and flexible Web interface, and we largely provide this in the form of interactive analysis and plotting tools which we will continue to improve in order to fulfill I3RC's educational objective.

(3) ***Portability***. Some of the participating codes have been ported to a common Linux computer. The open source initiative within I3RC will require that all submitted code be tested with the Portland Fortran compiler available there. Some routines will be selected for porting to a multiprocessing environment. Maintaining portability will be an important ongoing effort, without which shared code would have limited usefulness.

(4) ***Scalability***. Input cloud fields for I3RC must have a spatial resolution capable of resolving typical photon mean-free-path on the order of 100 meters, in order to represent 3D radiation effects, yet cover a sufficiently large domain to fairly represent cloud variability unresolved by GCMs, currently exceeding ~50 km horizontally. These two goals are not simultaneously achievable at present with commonly available computing resources. The I3RC baseline cases

handle this problem by choosing relatively small domains within which 3D effects are well-resolved, and assuming that plane-parallel biases in domain-averaged quantities can be scaled up to the larger scales needed by models. This relies on empirical and cloud-resolving modeling studies of the scaling properties of clouds, that are still ongoing.

I3RC has provided a focus for radiation scientists working on applications to cloudy atmospheres, similar to what RAMI has provided for applications to vegetation. These two efforts are now beginning to converge, along with parallel efforts relating to 3D transfer in sea ice, snow, and other components of the climate system. For this purpose a new 3D RT working group has been organized, chaired by one of the authors (Cahalan) and sponsored by the IRC. The 3D RT group is coordinated by an executive committee that comes from a cross section of the 3D RT community. The group hopes to share tools and insights gleaned from the variety of applications in which they are engaged, and to encourage and enable the extension of 3DRT to new applications in earth science.

We are looking forward to a greater exposure of graduate students to the world of 3D atmospheric radiation in academic curricula, and the imminent publication of the first monograph exclusively dedicated to the subject ("Three Dimensional Radiative Transfer in the Cloudy Atmosphere", Springer-Verlag, Marshak and Davis eds., 2004) will definitely help in that regard. There will then be an even greater audience to which we can voice our belief that a bright future lies ahead for 3D RT in climate research and remote sensing alike. While 3D RT models are by no means perfect or in perfect agreement, they have been steadily converging toward common answers, so investigation of approaches that would make them suitable for routine meteorological and climatic applications should intensify. Our hope is that the I3RC project will be viewed as one of the main contributors to the advancement of the field of atmospheric radiation.

*Acknowledgements*. I3RC received financial support by DoE via interagency agreement DE-AI02-00ER62939 and under NASA grants 621-30-86, 622-42-57. We appreciate the support and encouragement of Tom Ackerman and Wanda Ferrell of the DOE/ARM Program, Don Anderson and Hal Maring of the NASA Radiation Sciences Program, Graeme Stephens and William Rossow of the GEWEX Radiation Panel, and Herbert Fisher and Robert Ellingson of the International Radiation Commission. We would also like to thank the 3D RT community at large for its remarkable efforts to advance the field in the last three decades.

## References


Barker, H. W., J.-J. Morcrette, and G. D. Alexander, 1998: Broadband solar fluxes and heating for atmospheres with 3D broken clouds. *Quart. J. Roy. Meteor. Soc.,* **124,** 1245–1271.

Barker, H. W., G. L. Stephens, and Q. Fu, 1999: The sensitivity of domain averaged solar fluxes to assumptions about cloud geometry. *Quart. J. Roy. Meteor. Soc.,* **125,** 2127–2152.

Barker, H. W., and coauthors, 2003: Assessing 1D atmospheric solar radiative transfer models: Interpretation and handling of unresolved clouds. *J. Climate*, **16**, 2,676-2,699.

Byrne, R. N., R. C. J. Somerville, and B. Subasilar, 1996: Broken-cloud enhancement of solar radiation absorption. *J. Atmos. Sci.*, **53**, 878-886.

Cahalan, R. F., Overview of Fractal Clouds, 1989: *Advances in Remote Sensing*. A. Deepak Publishing, 515 pp., 371-388.

Cahalan, R. F., W. Ridgway, W. J. Wiscombe, S. Gollmer, and Harshvardhan, 1994: Independent pixel and Monte Carlo estimates of stratocumulus albedo. *J. Atmos. Sci.,* **51,** 3776–3790.

Cahalan, R. F., and R. Davies (eds.), 2000: *Intercomparison of three-dimensional radiation codes: Abstracts of the first and second international workshops*. University of Arizona Press, Tucson (AZ), ISBN 0-9709609-0-5.

Cess, R. D., and co-authors 1989: Interpretation of cloud-climate feedback as produced by 14 atmospheric general circulation models. *Science,* **245**, 513-515.

Cess, R. D., and co-authors, 1990: Intercomparison and interpretation of climate feedback processes in 19 atmospheric general circulation models. *J. Geophys. Res.,* **95**, 16,601-16,615.

Cess, R. D., and coauthors, 1996: Cloud feedback in atmospheric general circulation models: An update. *J. Geophys. Res.,* **101**, 12,791-12,794.

Chambers, L., B. Wielicki, and K.F. Evans, 1997: On the accuracy of the independent pixel approximation for satellite estimates of oceanic boundary layer cloud optical depth. *J. Geophys. Res.*, **102**, 1779-1794.

Davies, R., 1978: The effect of finite cloud geometry on the 3D transfer of solar irradiance in clouds, J. Atmos. Sci. 35, 1712-1725.

Davis, A. B. and A. Marshak, 2001): Multiple scattering in clouds: Insights from three-dimensional diffusion/$P_1$ theory. *Nuclear Sci. and Engin.*, **137**, 251–280.

Evans, K.F. (1998). The spherical harmonics discrete ordinate method for three-dimensional atmospheric radiative transfer. *J. Atmos. Sci.*, **55**, 429–446.

Fu, Q., S. K. Krueger, and K.-N. Liou, 1995: Interactions of radiation and convection in simulated tropical cloud clusters. *J. Atmos. Sci.*, **52**, 1310-1328.

Kassianov, E., T. Ackerman, R. Marchand and M. Ovtchinnikov, 2003: Stochastic radiative transfer in multilayer broken clouds - Part II: Validation tests. *J. Quant. Spectrosc. Radiat. Transfer*, **77**, 395–416.

Kiehl, J.T. and K.E. Trenberth, 1997: Earth’s annual global mean energy budget. *Bull. Amer. Meteor. Soc.*, **78**, 197–208.

Marchuk, G., G. Mikhailov, M. Nazaraliev, R. Darbinjan, B. Kargin and B. Elepov, 1980: *The Monte Carlo Methods in Atmospheric Optics*. Springer-Verlag, New York (NY).

Marshak., A., A. Davis, W. Wiscombe, and R. F. Cahalan, 1995: Radiative smoothing in fractal clouds. *J. Geophys. Res.*, **100**, 26,427-26,261.

Marshak, A., L. Oreopoulos, A. Davis, W. Wiscombe and R. Cahalan, 1999: Horizontal radiative fluxes in clouds and accuracy of the Independent Pixel Approximation at absorbing wavelengths. *Geophys. Res. Lett.*, **11**, 1585–1588.

McKee, T. B. and S. K. Cox, 1974: Scattering of visible radiation by finite clouds. *J. Atmos. Sci.*, **31**, 1885–1892.

Moeng, C.-H., and coauthors, 1996: Simulation of a stratocumulus-topped planetary boundary layer: Intercomparison among different numerical codes. *Bull. Am. Meteor. Soc.* **77**, 261–278.

Mullamaa, Y. R., M. A. Sulev, V. K. Poldmaa, H. A. Ohvril, H. J. Nrylisk, M. I. Allenov, L. G. Tchuhakov, and A. F. Kuusk, 1972: Stochastic structure of cloud and radiation fields. *Academy of Sciences of Estonian SSR, NASA Technical Translation TT F-822*, 1975, 1–192.

Oreopoulos, L., and R. Davies, 1998: Plane parallel albedo biases from satellite observations. Part I: Dependence on resolution and other factors. *J. Climate* , **11** , 919-932.

Pinty, B., and coauthors, 2001: The radiation transfer model intercomparison (RAMI) exercise. *J. Geophys. Res.*, **106**, 11,937-11,956.

Pinty, B., and coauthors, 2004: The radiation transfer model intercomparison (RAMI) exercise: Results from the second phase. *J. Geophys. Res.*, **109**, doi: 10.1029/2003JD004252.

Ramanathan, V., R.D. Cess, E.F. Harrison, P. Minnis, B.R. Barkstrom, E. Ahmad and D. Hartmann, 1989: Cloud-radiative forcing and climate: Results from the Earth-radiation Budget Experiment. *Science*, **243**, 57–63.

Randall, D., M. Khairoutdinov, A. Arakawa and W. Grabowski, 2003: Breaking the cloud parameterization deadlock. *Bull. Amer. Meteor. Soc.*, **84**, 1547–1564.

Stamnes, K., S.-C. Tsay, W. J. Wiscombe and K. Jayaweera, 1988. Numerically stable algorithm for discrete-ordinate-method radiative transfer in multiple scattering and emitting layered media. *Appl. Opt.*, **27**, 2502–2509.

Stevens, B., D. H. Lenschow, 2001: Observations, experiments, and Large Eddy Simulation. *Bull. Amer. Meteor. Soc.*, **82**, 283–294.

Várnai, T., and R. Davies, 1999: Effects of cloud heterogeneities on shortwave radiation: comparison of cloud-top variability and internal heterogeneity. *J. Atmos. Sci.*, **56**, 4206-4224.

Várnai, T. and A. Marshak, 2002: Observations and analysis of 3-dimensional radiative effects that influence MODIS cloud optical thickness retrievals. *J. Atmos. Sci.*, **59**, 1607-1618.

**Table 1**

| # | Code | Institution | Contact Person | Country | Method Description |
|---|---|---|---|---|---|
| 1 | ARIZ | Formerly University of Arizona, now at UCLA | M. Garay | USA | Monte Carlo |
| 2 | COLS | Colorado State University | P. Partain | USA | Monte Carlo |
| 3 | IAOT | Institute of Atmospheric Optics | T. Zhuravleva | Russia | Monte Carlo |
| 4 | IMCL | Imperial College of London | N. Trasi | United Kingdom | Modified Even-parity Neutron Transport Code (EVENT) |
| 5 | KIAE1 | Kurchatov Institute | A. Rublev | Russia | Monte Carlo |
| 6 | KIAE2 | Kurchatov Institute | A. Rublev | Russia | Monte Carlo using adjoint RT equation |
| 7 | LANL1 | Los Alamos National Laboratory | A. Davis | USA | TWODANT(Diffusion accelerated Discr. Ordinates) |
| 8 | LANL2 | Los Alamos National Laboratory | A. Davis | USA | Discrete Angles (6-beam model, using Monte Carlo) |
| 9 | LANL3 | Los Alamos National Laboratory | A. Davis | USA | ED3D (3D Delta- Eddington) |
| 10 | MESC1 | Meteorological Service Of Canada | H. Barker | Canada | Monte Carlo |
| 11 | MESC2 | Meteorological Service Of Canada | H. Barker | Canada | Monte Carlo, Delta-scaled Optical Properties |
| 12 | NCAR | Formerly NCAR, now DLR | B. Mayer | Germany | Monte Carlo, libRadtran |
| 13 | PENN | The Pennsylvania State University | E. Clothiaux | USA | Monte Carlo, Max. Cross |
| 14 | PNNL | Pacific Northwest National Laboratory | E. Kassianov | USA | Monte Carlo, Max. Cross Section |
| 15 | UCOL1 | University of Colorado | K. F. Evans | USA | SHDOM, Low Resolution |
| 16 | UCOL2 | University of Colorado | K. F. Evans | USA | SHDOM, High Resolution |
| 17 | UCSB | University of California Santa Barbara | W. O'Hirok | USA | Monte Carlo |
| 18 | UMBC1 | University of Maryland Baltimore County | A. Marshak | USA | Monte Carlo, Local Max. Cross Section |
| 19 | UMBC2 | University of Maryland Baltimore County | T. Varnai | USA | Monte Carlo, Max. Cross Section |
| 20 | UMBC3 | Formerly UMBC, now at Max Planck Institute | S. Kinne | USA | Monte Carlo |
| 21 | UMBC4 | Formerly UMBC, now at Max Planck Institute | S.Kinne | USA | Discrete Angles (6-beam model, using relaxation) |
| 22 | UNBP | Université Blaise Pascal | F. Szczap | France | Neural networks (radiances) |
| 23 | UNIK | University of Kiel | A. Macke | Germany | Monte Carlo |

**Table 2**

| # | Code | Institution | Contact Person | Country | Method Description |
|---|---|---|---|---|---|
| 1 | ARIZ | Formerly University of Arizona, now at UCLA | M. Garay | USA | Monte Carlo |
| 2 | DZLR1 | Deutsches Zentrum für Luft und Raumfahrt | B. Mayer | Germany | Monte Carlo, libRadtran |
| 3 | DZLR2 | Deutsches Zentrum für Luft und Raumfahrt | B. Mayer | Germany | Monte Carlo, libRadtran truncated forward peak |
| 4 | IAOT | Institute of Atmospheric Optics | T. Zhuravleva | Russia | Monte Carlo, Max. Cross Section |
| 5 | ICOM | Institute of Computational Mathematics | S. Prigarin | Russia | Monte Carlo, Max. Cross Section |
| 6 | PENN | The Pennsylvania State University | E. Clothiaux | USA | Monte Carlo, Max. Cross Section |
| 7 | PNNL | Pacific Northwest National Laboratory | E. Kassianov | USA | Monte Carlo |
| 8 | UCOL | University of Colorado | F. Evans | USA | SHDOM |
| 9 | UCSB | University of California Santa Barbara | W. O'Hirok | USA | Monte Carlo |
| 10 | UMBC1 | University of Maryland Baltimore County | A. Marshak | USA | Monte Carlo, Local Max. Cross Section |
| 11 | UMBC5 | University of Maryland Baltimore County | T. Varnai | USA | Monte Carlo, Max. Cross Section |
| 12 | UMCP | Formerly University of Maryland, College Park, now at FSU | E. Takara | USA | Monte Carlo, LW, backward |
| 13 | UNIK | University of Kiel | A. Macke | Germany | Monte Carlo |

**Table 3**

| Description | Contact Person(s), Institution(s) | I3RC Status |
|---|---|---|
| Direct-Beam IPA | K. F. Evans (UCOL), P. Gabriel (COLS) | * |
| Tilted IPA | T. Varnai (UMBC), R. Davies (JPL) | * |
| Nonlocal IPA | A. Marshak (NASA), L. Oreopoulos (UMBC) | * |
| Mapping Neural Networks | F. Szczap (LAMP), C. Comet (LOA) | * |
| Successive orders-of-scattering | R. Davies (JPL), M. Garay (UCLA) | * |
| Diffusion, finite differences (ED3D) | Z. Qu (CIRES), A. Davis (LANL) | * |
| Diffusion, finite differences | Y. Chen (UCLA), K.-N. Liou (UCLA) | * |
| Diffusion, finite elements | A. Davis (LANL), M. Hall (LANL) | * |
| EVENT truncated at $L$= 1 | N. Trasi (IMCL), C. de Oliveira (IMCL) | * |
| SHDOM truncated at $L$=1 | K. F. Evans (UCOL) | |
| DA, Monte Carlo | A. Davis (LANL) | * |
| DA, 1st-order, relaxation | S. Kinne (UMBC) | * |
| DA, 2nd-order, finite elements | A. Davis (LANL), C. Rohde (LANL) | * |
| 2nd-order adjoint perturbation | M. Box (UNSW), I. Polonsky (LANL) | * |

**Table 4**

| Description | Contact Person(s), Institution(s) | I3RC status |
|---|---|---|
| Effective optical thickness | R. F. Cahalan (GSFC) | * |
| Gamma-ICA | H. W. Barker (MESC), L. Oreopoulos (UMBC) | * |
| Anomalous/Levy diffusion | A. Davis (LANL), A. Marshak (UMBC) | * |
| Stochastic radiative transfer | D. Veron (Rutgers), N. Byrne (SAIC) | * |
| Stochastic radiative transfer | T. Zhuravleva (IAOT) | * |
| Stochastic RT, multi-stream | Y.-X. Hu (LARC) | ? |
| Stochastic RT, 2-stream | Y.-X. Hu (LARC), A. Davis (LANL) | * |
| "New optical properties" | G. Stephens, P. Gabriel (COLS) | ? |
| Renormalization | B. Cairns (GISS) | ? |
| "Cloudlets" | G. Petty (U. Wisconsin - Madison) | ? |
| Monte Carlo-ICA | H. Barker (MESC), R. Pincus (NOAA-CIRES) | ? |
| Multi-layer cloud stochastic | E. Kassianov (PNNL) | ? |

## Figure Captions

**Figure 1** Integrated visible optical thickness for the three cloud fields of I3RC Phase I: Case 1, called “step cloud” (top); Case 2, based on millimeter radar observations (middle); and Case 3 based on retrievals from high resolution Landsat radiance measurements (bottom).

**Figure 2** Reflectance ($R$), transmittance ($T$), absorptance ($A$) and horizontal flux $H$=1-$R$-$T$-$A$ for experiment 4, case 1 of Phase I (“step cloud”) from 18 participating codes. The single scattering albedo (probability of a photon surviving after an interaction with the cloud particle) is 0.99, the scattering phase function is that of Henyey-Greenstein with asymmetry factor (mean cosine of the scattering angle) $g$=0.85, the solar zenith angle is 60° (Sun shining from left), the surface is black (non-reflecting), and periodic boundary conditions in the horizontal are used. Only outliers are identified (see Table 1).

**Figure 3** Nadir radiance (bidirectional reflectance) fields of selected submissions for experiment 4 of case 3 (the Landsat field of Fig. 1) of I3RC Phase I. The input parameter values are the same as in the step cloud case shown in Fig. 2. The colors represent a range of values extending from 0 (black) to 0.8 (red). It can be seen that all participants capture the main spatial features of the radiance field, while for the MC fields (all but UCOL1) the noisiness of the field is a function of the number of photons used and the method of radiance calculation, i.e., “cone” method (e.g., Várnai and Davies, 1999) vs. “local estimate” method (e.g., Marshak et al., 1995). Even the noisest of the submissions manage to capture the mean radiance field quite accurately (Fig. 4).

**Figure 4** Domain-average nadir reflectivity (gray bars) and standard deviation (black bars) for all models that participated in the I3RC Phase I experiment shown in the previous figure.

**Figure 5** Top-down view of integrated visible optical thickness field for the two LES cloud fields of I3RC Phase II: cumulus (top) and stratocumulus (bottom).

**Figure 6** High-accuracy nadir reflectance fields for the LES Cumulus cloud field of Phase II. The colors represent a range of values extending from 0 (violet) to 1.2 (red). This is experiment 7 which includes an absorbing and scattering atmosphere consisting of aerosols and gases, a reflecting Lambertian surface of 0.2 albedo, and assumes a Mie phase function for the scattering particles (spherical liquid droplets, non-absorbing for this experiment). The sun is at a solar zenith angle of 60° and is shining from the left side of the domain.

**Figure 7** Domain-average nadir reflectivity (gray bars) and standard deviation (black bars) for the fields shown in Fig. 6.

**Figure 8** The interface of the interactive plot tool in the I3RC website (http://i3rc.gsfc.nasa.gov) for summary statistics (top) and cross-comparison statistics (bottom).

**Figure 9** The interface of the interactive plot tool in the I3RC website (http://i3rc.gsfc.nasa.gov) for creating 2D images and 1D transects of radiation fields.

## List of Tables

## List of Acronyms

**ARIZ:** University of Arizona

**CDC:** Climate Diagnostics Center

**CIRES:** Cooperative Instrument for Research in Environmental Sciences

**COLS:** Colorado State

**CPU:** Central Processing Unit

**CRM:** Cloud Resolving Model

**DA:** Discrete Angle

**DZLR:** Deutsches Zentrum für Luft und Raumfahrt

**ED3D:** Eddington-Delta in 3D

**EOS:** Earth Observing System

**EVENT:** Even-parity Neutron Transport

**GCM:** General Circulation Model

**GISS:** Goddard Institute for Space Studies

**GSFC:** Goddard Space Flight Center

**IAOT:** Institute of Atmospheric Optics at Tomsk

**ICOM:** Institute of Computational Mathematics

**ICRCCM:** Intercomparison of Radiation Codes in Climate Models

**IMCL:** Imperial College of London

**IRC:** International Radiation Commission

**I3RC:** International Intercomparison of 3D Radiation Codes (http://i3rc.gsfc.nasa.gov)

**IPA:** Independent Pixel Approximation

**ICA:** Independent Column Approximation

**JPL:** Jet Propulsion Laboratory

**KIAE:** Kurchatov Institute

**LAMP:** Laboratoire de Meteorologie Physique

**LANL:** Los Alamos National Laboratory

**LARC:** NASA Langley Research Center

**LES:** Large Eddy Simulation

**LOA:** Laboratoire d' Optique Atmospherique

**MC:** Monte Carlo

**MESC:** Meteorological Service of Canada

**MMF:** Multi-Scale Modelling Framework

**NCAR:** National Center for Atmospheric Research

**NOAA:** National Oceanic and Atmospheric Administration

**PENN:** Penn State

**PNNL:** Pacific Northwest National Laboratory

**RAMI:** Radiation Transfer Model Intercomparison

**RT:** Radiative Transfer

**RTE:** Radiative Transfer Equation

**SAIC:** Science Applications International Corporation

**SHDOM:** Spherical Harmonics Discrete Ordinate Method

**UCLA:** University of California Los Angeles

**UCOL:** University of Colorado

**UCSB:** University of California Santa Barbara

**UMBC:** University of Maryland Baltimore County

**UNIK:** University of Kiel

**UNSW:** University of New South Wales

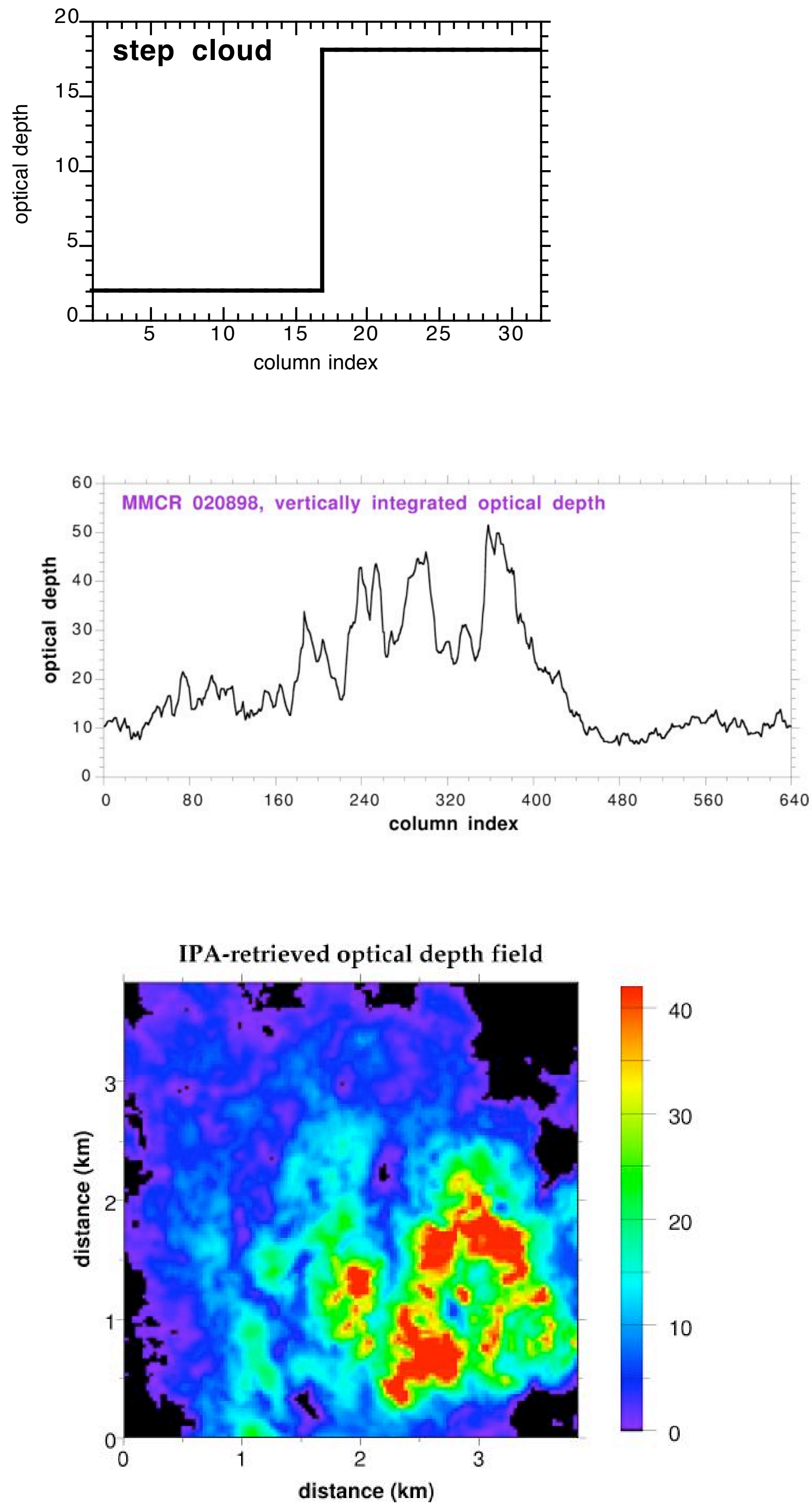
step cloud
optical depth
column index
MMCR 020898, vertically integrated optical depth
optical depth
column index
IPA-retrieved optical depth field
distance (km)
distance (km)

**Figure 1**

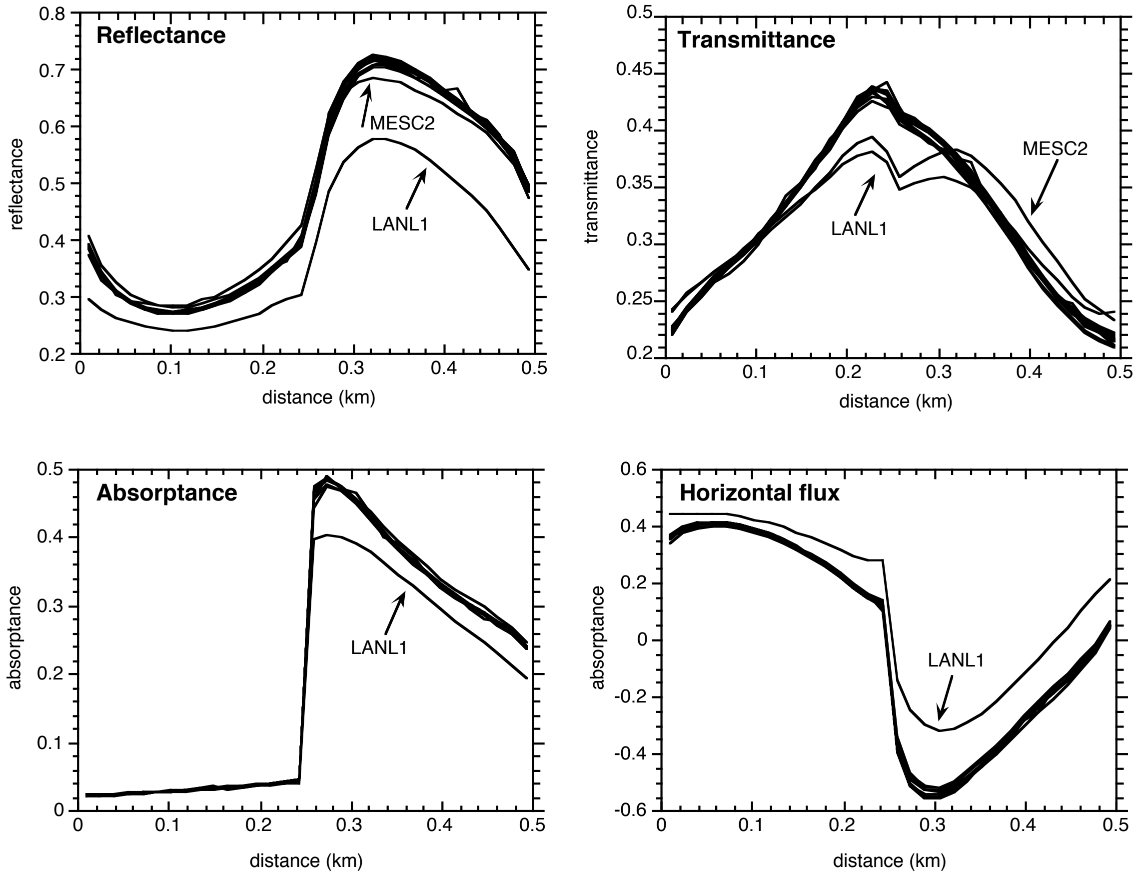
Reflectance
reflectance
MESC2
LANL1
distance (km)
Transmittance
transmittance
MESC2
LANL1
distance (km)
Absorptance
absorptance
LANL1
distance (km)
Horizontal flux
absorptance
LANL1
distance (km)

**Figure 2**

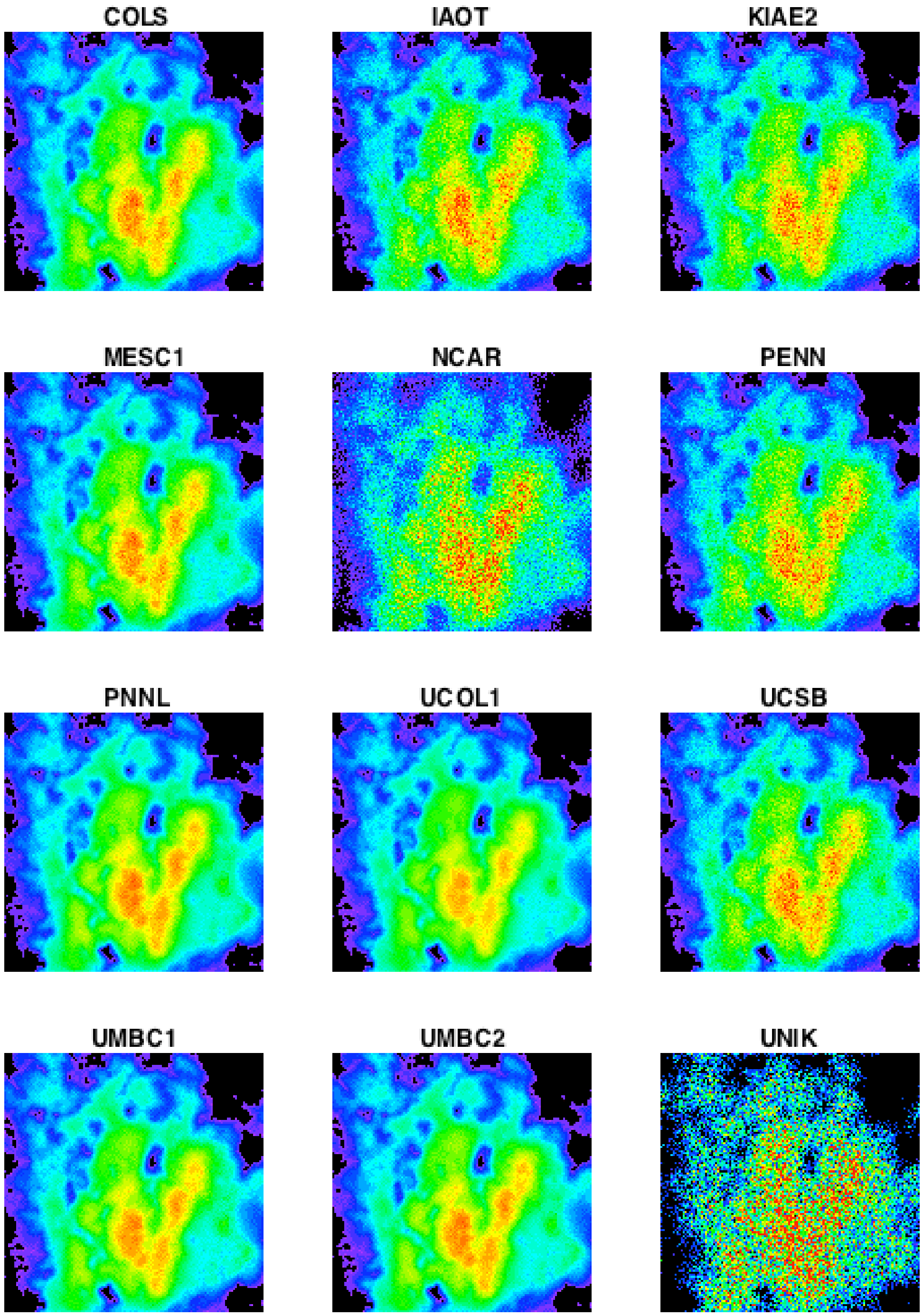
COLS
IAOT
KIAE2
MESC1
NCAR
PENN
PNNL
UCOL1
UCSB
UMBC1
UMBC2
UNIK

**Figure 3**

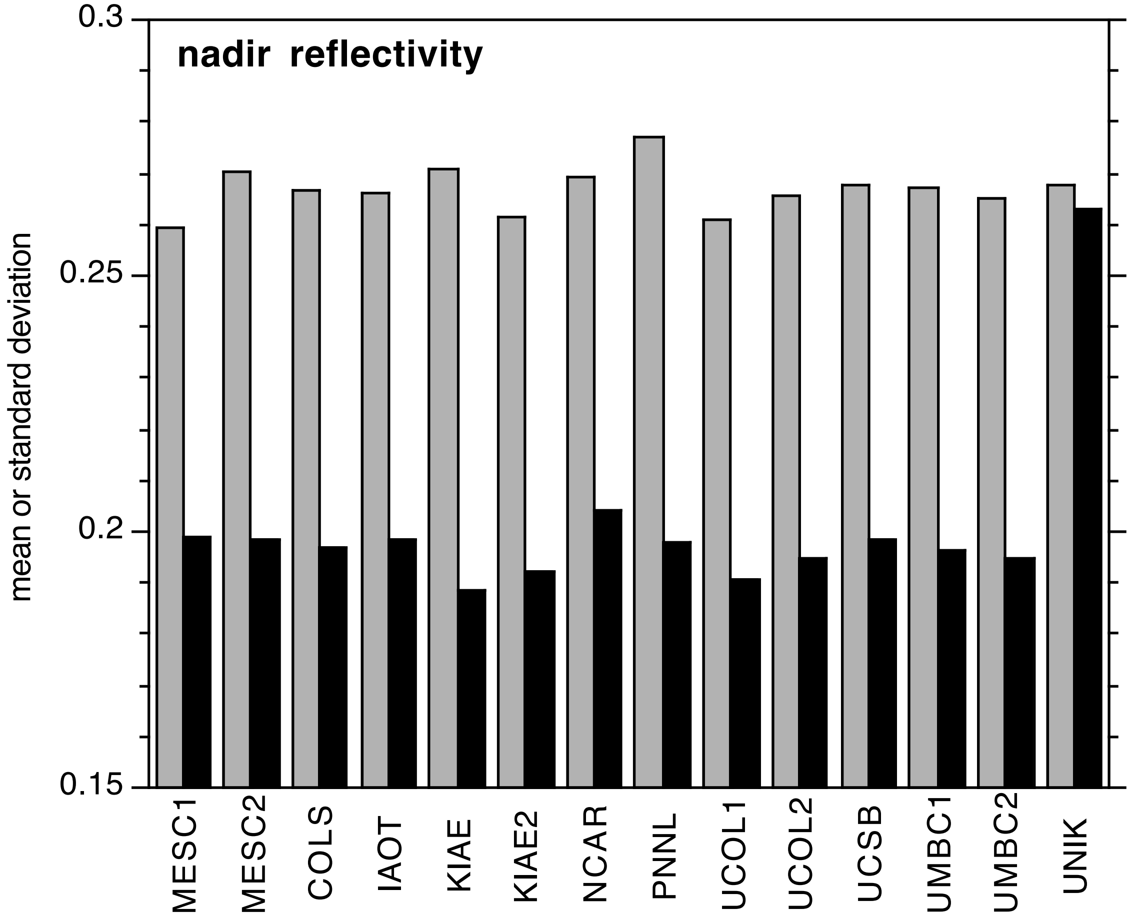
0.3
0.25
0.2
0.15
mean or standard deviation
nadir reflectivity
MESC1
MESC2
COLS
IAOT
KIAE
KIAE2
NCAR
PNNL
UCOL1
UCOL2
UCSB
UMBC1
UMBC2
UNIK

**Figure 4**

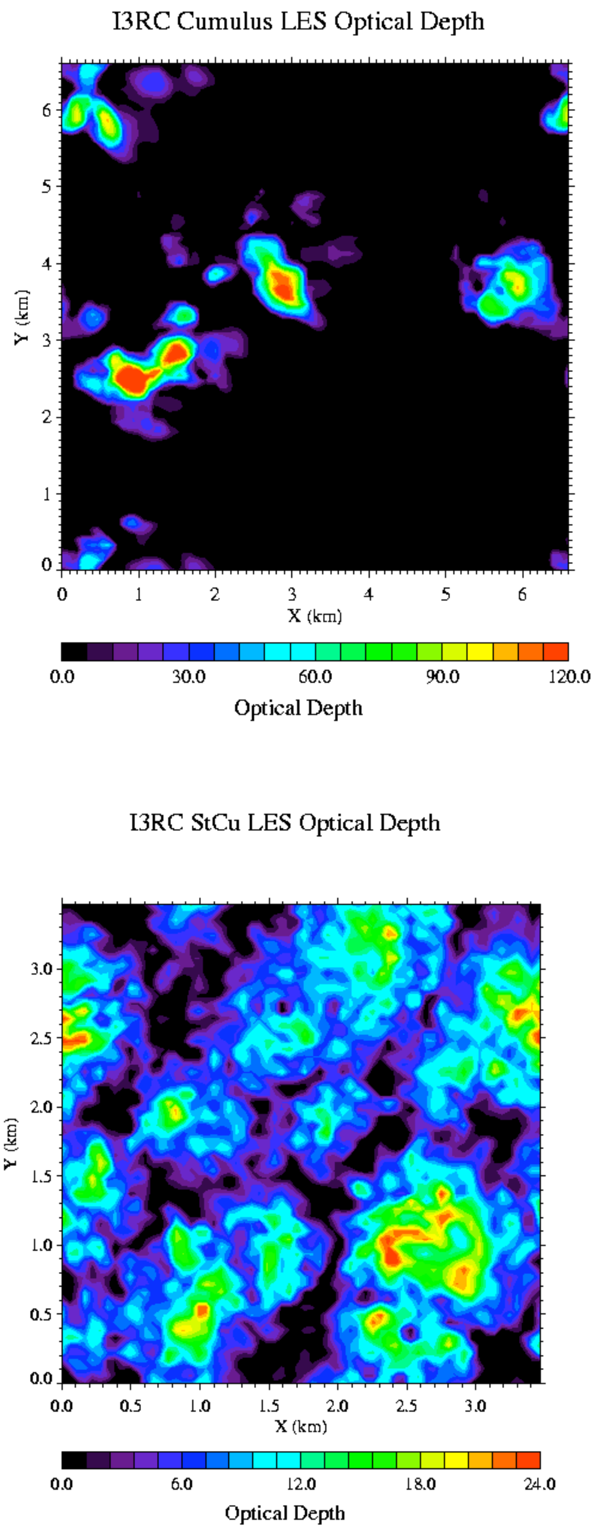
I3RC Cumulus LES Optical Depth
Y (km)
X (km)
0.0
30.0
60.0
90.0
120.0
Optical Depth
I3RC StCu LES Optical Depth
Y (km)
X (km)
0.0
6.0
12.0
18.0
24.0
Optical Depth

**Figure 5**

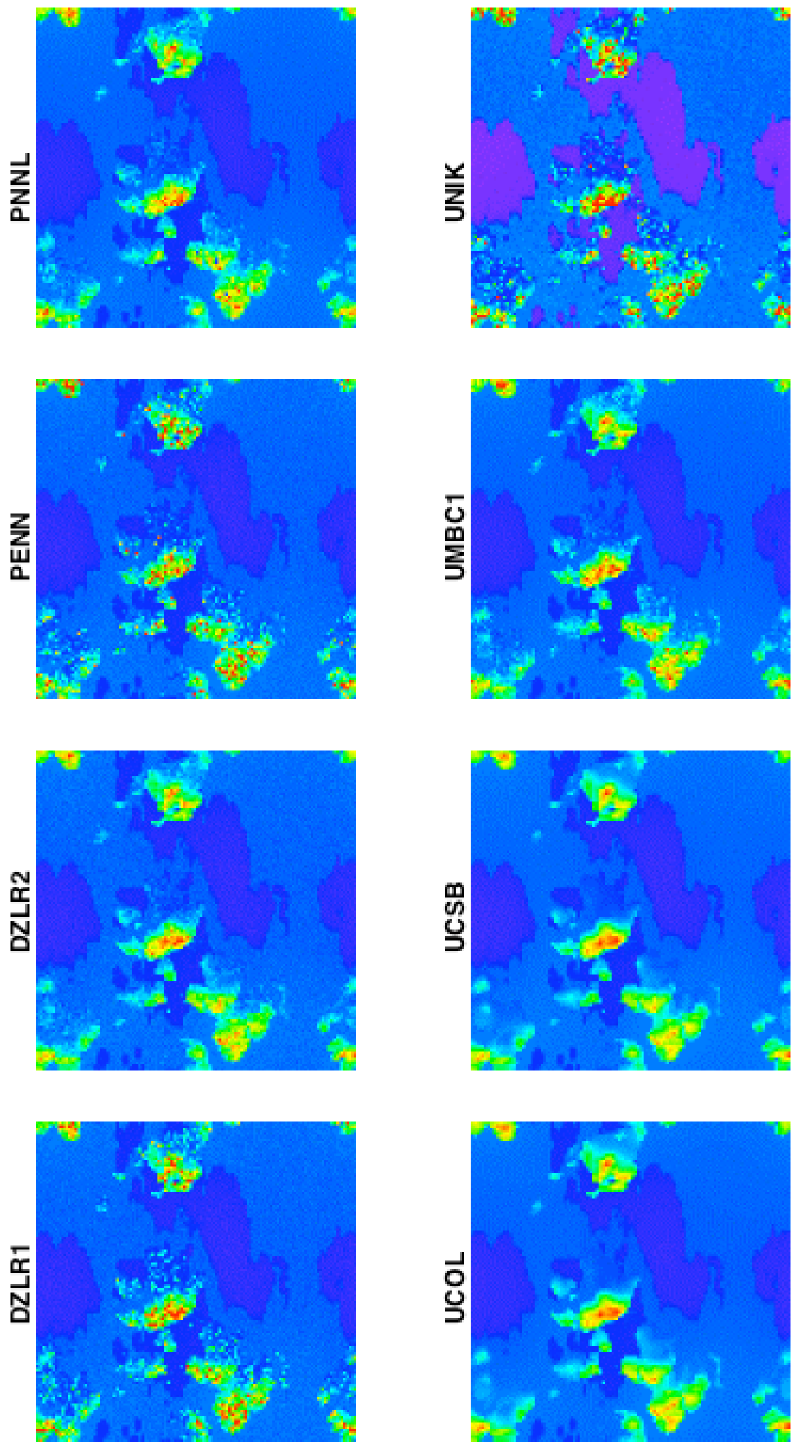


**Figure 6**

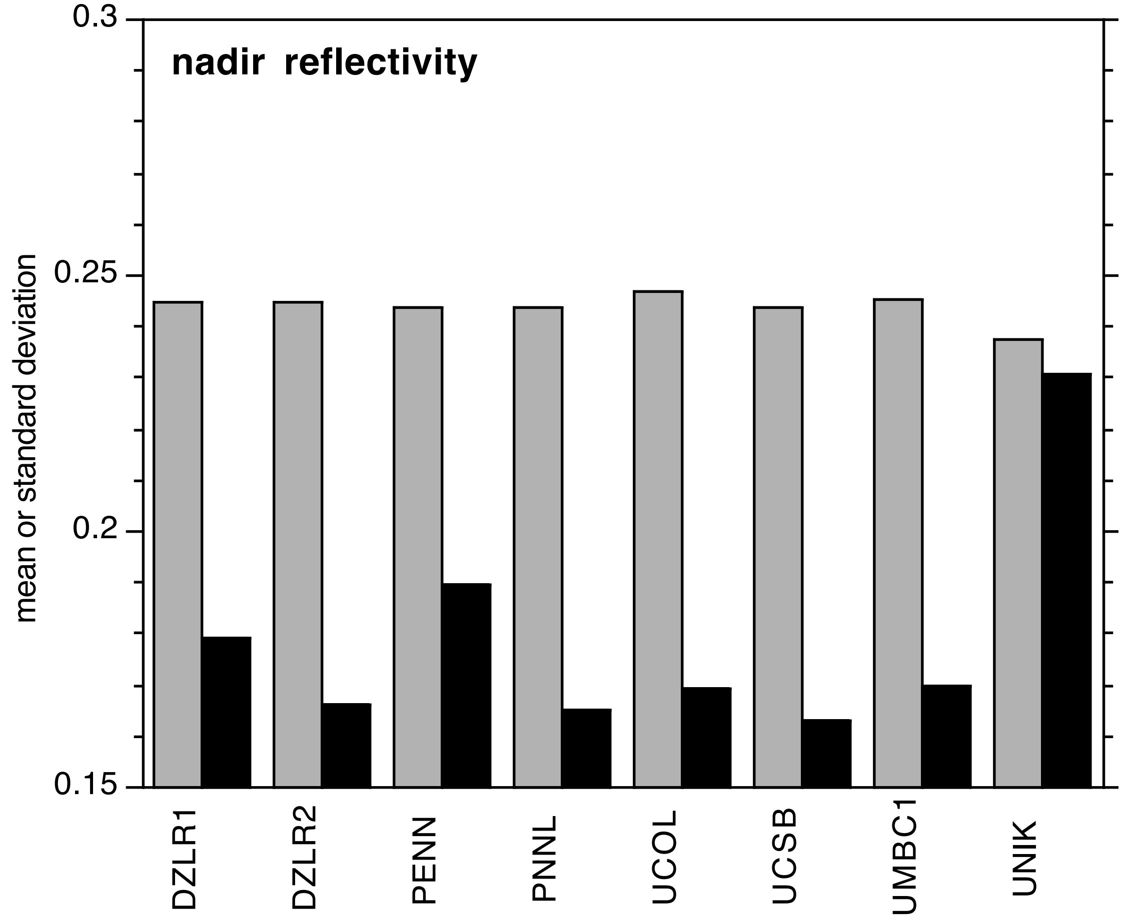
nadir reflectivity
mean or standard deviation
0.3
0.25
0.2
0.15
DZLR1
DZLR2
PENN
PNNL
UCOL
UCSB
UMBC1
UNIK

**Figure 7**

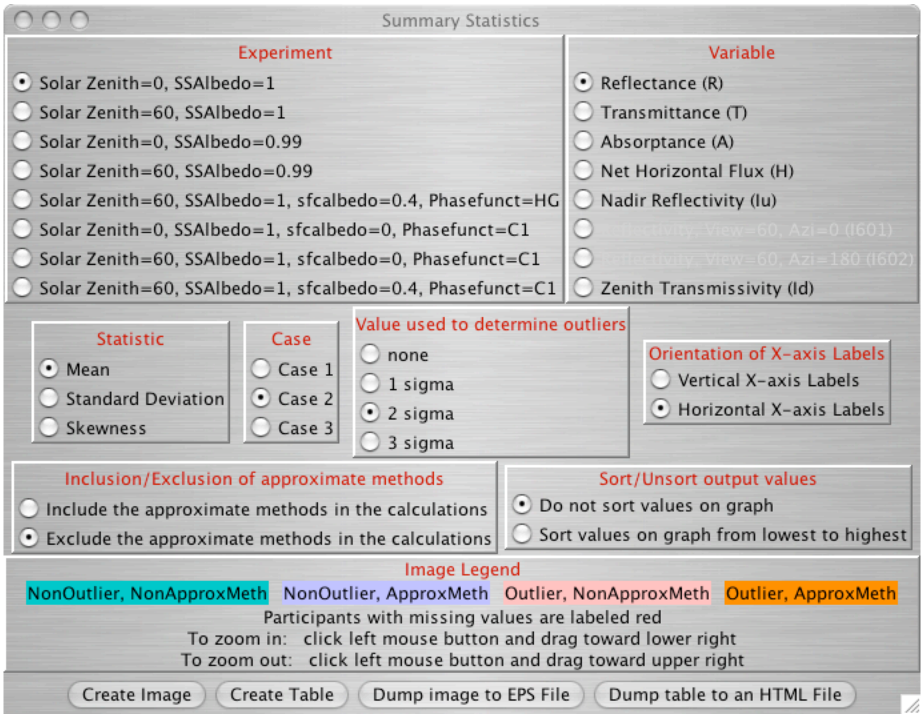
Summary Statistics
Experiment
Solar Zenith=0, SSAlbedo=1
Solar Zenith=60, SSAlbedo=1
Solar Zenith=0, SSAlbedo=0.99
Solar Zenith=60, SSAlbedo=0.99
Solar Zenith=60, SSAlbedo=1, sfcalbedo=0.4, Phasefunct=HG
Solar Zenith=0, SSAlbedo=1, sfcalbedo=0, Phasefunct=C1
Solar Zenith=60, SSAlbedo=1, sfcalbedo=0, Phasefunct=C1
Solar Zenith=60, SSAlbedo=1, sfcalbedo=0.4, Phasefunct=C1
Variable
Reflectance (R)
Transmittance (T)
Absorptance (A)
Net Horizontal Flux (H)
Nadir Reflectivity (Iu)
Zenith Transmissivity (Id)
Statistic
Mean
Standard Deviation
Skewness
Case
Case 1
Case 2
Case 3
Value used to determine outliers
none
1 sigma
2 sigma
3 sigma
Orientation of X-axis Labels
Vertical X-axis Labels
Horizontal X-axis Labels
Inclusion/Exclusion of approximate methods
Include the approximate methods in the calculations
Exclude the approximate methods in the calculations
Sort/Unsort output values
Do not sort values on graph
Sort values on graph from lowest to highest
Image Legend
NonOutlier, NonApproxMeth
NonOutlier, ApproxMeth
Outlier, NonApproxMeth
Outlier, ApproxMeth
Participants with missing values are labeled red
To zoom in: click left mouse button and drag toward lower right
To zoom out: click left mouse button and drag toward upper right
Create Image
Create Table
Dump image to EPS File
Dump table to an HTML File

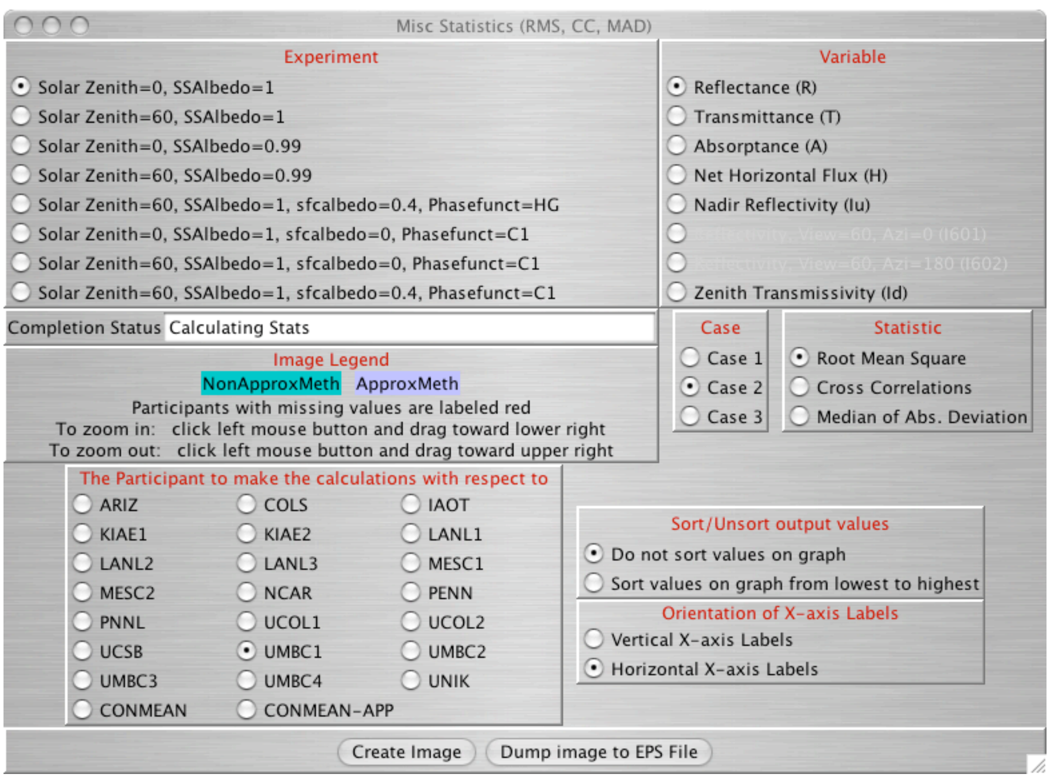
Misc Statistics (RMS, CC, MAD)
Experiment
Solar Zenith=0, SSAlbedo=1
Solar Zenith=60, SSAlbedo=1
Solar Zenith=0, SSAlbedo=0.99
Solar Zenith=60, SSAlbedo=0.99
Solar Zenith=60, SSAlbedo=1, sfcalbedo=0.4, Phasefunct=HG
Solar Zenith=0, SSAlbedo=1, sfcalbedo=0, Phasefunct=C1
Solar Zenith=60, SSAlbedo=1, sfcalbedo=0, Phasefunct=C1
Solar Zenith=60, SSAlbedo=1, sfcalbedo=0.4, Phasefunct=C1
Variable
Reflectance (R)
Transmittance (T)
Absorptance (A)
Net Horizontal Flux (H)
Nadir Reflectivity (Iu)
Zenith Transmissivity (Id)
Completion Status
Calculating Stats
Case
Case 1
Case 2
Case 3
Statistic
Root Mean Square
Cross Correlations
Median of Abs. Deviation
Image Legend
NonApproxMeth
ApproxMeth
Participants with missing values are labeled red
To zoom in: click left mouse button and drag toward lower right
To zoom out: click left mouse button and drag toward upper right
The Participant to make the calculations with respect to
ARIZ
COLS
IAOT
KIAE1
KIAE2
LANL1
LANL2
LANL3
MESC1
MESC2
NCAR
PENN
PNNL
UCOL1
UCOL2
UCSB
UMBC1
UMBC2
UMBC3
UMBC4
UNIK
CONMEAN
CONMEAN-APP
Sort/Unsort output values
Do not sort values on graph
Sort values on graph from lowest to highest
Orientation of X-axis Labels
Vertical X-axis Labels
Horizontal X-axis Labels
Create Image
Dump image to EPS File

**Figure 8**


Phase I fields
Case
CASE 1
CASE 2
CASE 3
Experiment
Solar Zenith=0, SSAlbedo=1
Solar Zenith=60, SSAlbedo=1
Solar Zenith=0, SSAlbedo=0.99
Solar Zenith=60, SSAlbedo=0.99
Solar Zenith=60, SSAlbedo=1, sfcalbedo=0.4, Phasefunct=HG
Solar Zenith=0, SSAlbedo=1, sfcalbedo=0, Phasefunct=C1
Solar Zenith=60, SSAlbedo=1, sfcalbedo=0, Phasefunct=C1
Solar Zenith=60, SSAlbedo=1, sfcalbedo=0.4, Phasefunct=C1
Variable
Reflectance (R)
Transmittance (T)
Absorptance (A)
Net Horizontal Flux (H)
Nadir Reflectivity (Iu)
Zenith Transmissivity (Id)
Information
Plot Type
X-Y Plot
2D Plot
Participants
Completion Status
Row 1
Orientation of X-axis Labels
Vertical X-axis Labels
Horizontal X-axis Labels
Select Participants to show on graph
ARIZ
COLS
IAOT
KIAE1
MESC1
MESC2
NCAR
PENN
PNNL
UCOL1
UCOL2
UCSB
UMBC1
UMBC2
UMBC3
UNIK
ALL PART.
Conmean
Conmean-App
Conmean-Out
Type of Plot
Basic Field Plot
Difference Field Plot
Select Participant to subtract from
Select output Participants
Type of CASE3 Display
Create a 1D cross section
Create a 2D display
Select row/column
Extract row
Extract col
1
25
50
75
100
128
Create Image
Dump image to EPS File

**Figure 9**